Incorporation of a Stilbazole Derivative in the Hydrogen-Bonded Chain of L-Tartrate: Toward a One-Step Optimization of Molecular and Bulk Second-Order Nonlinearities

Pascal G. Lacroix* and Jean Claude Daran

Laboratoire de Chimie de Coordination, CNRS, 205 route de Narbonne, 31077 Toulouse Cedex, France

Keitaro Nakatani

P.P.S.M., Ecole Normale Supérieure de Cachan (P.P.S.M.), U.R. 1906, Avenue du Président Wilson, 94235 Cachan, France

Received October 22, 1997

The syntheses and crystal structures of dimethylaminostilbazole (DAS) and dimethylamino-*N*-methyl stilbazolium hydrogen L-tartrate (DAS-H^+Ta^-) are described. Crystal data for DAS: monoclinic, $P2_1/c$, $a = 6.0443(9)$ Å, $b = 7.6616(8)$ Å, $c = 26.376(4)$ Å, $\beta = 93.66(1)°$, $Z = 4$. Crystal data for DAS-H^+Ta^-: monoclinic, $P2_1$, $a = 7.518(1)$ Å, $b = 7.528(1)$ Å, $c = 16.376(2)$ Å, $\beta = 92.67(1)°$, $Z = 2$. In the latter compound, the anions create infinite chains through intermolecular O−H···O hydrogen bonds, whereas the stilbazolium cations are hydrogen bonded to the chains. INDO calculations and spectroscopic studies show that hydrogen bonding greatly enhances the molecular hyperpolarizability of the stilbazole derivative, while crystal engineering with tartaric acid is achieved into the acentric space group. Therefore, an efficiency of 8 times that of urea in second-harmonic generation has been measured at 1.907 μm for this material.

Introduction

The design and synthesis of organic materials exhibiting large second-order nonlinear optical (NLO) properties has been motivated by their potential for use in applications including telecommunications, optical computing, and optical data storage.[1,2] A generally successful and popular approach toward such materials is achieved in two steps which imply first the synthesis of extended conjugated systems with donor and acceptor groups that can ensure the largest known second-order molecular hyperpolarizability (β) of any class of materials. However, the molecular nonlinearity associated with a chromophore will lead to observable bulk nonlinearity (χ^2) only if the chromophores are oriented in a noncentrosymmetric environment.[3] To achieve this second step, the most popular strategy is the poled polymer approach, in which the polarizable chromophores are covalently bonded to the polymer and aligned by a strong electric field above the glass transition temperature (Tg) of the films.[4−6] On the other hand, the degree of alignment is very limited in this approach, which requires polymers with high Tg and chromophores exhibiting a good thermal stability.

To avoid these problems, alternative methods have been also investigated, usually based on the exploitation of molecular self-assembly (most notably crystal growth, incorporation into inclusion compounds, and formation of liquid crystal domains). On the other hand, the development of single-crystal NLO materials is hamped by the absence of general rules for predicting crystal structure from molecular structure.[7] Some progress has been made in this area exploiting hydrogen bonding.[8−13] Among these studies several are based on L-tartaric

(1) (a) *Molecular nonlinear Optics*; Zyss, J., Ed.; Academic: New York 1994. (b) *Organic Molecules for Nonlinear Optics and Photonics*; Messier J., Kajzar F., Prasad, P. Eds.; Kluwer Academic Publishers: Dordrecht, 1991. (c) *Introduction to Nonlinear Optical Effects in Molecules and Polymers*; Prasad, N. P., Williams, D. J., Eds.; Wiley: New York, 1991; pp 160−174.

(2) For recent reviews, see: (a) Dalton, L. R.; Harper, A. W.; Ghosn, R.; Steier, W. H.; Ziari, M.; Fetterman, H.; Shi, Y.; Mustacich, R. V.; Jen, A. K. Y. Shea, K. J. *Chem. Mater.* **1995**, *7*, 1060. (b) Benning, R. G. *J. Mater. Chem.* **1995**, *5*, 365. (c) *Optical nonlinearities in Chemistry*; Burland, D. M., Ed.; *Chem. Rev.* **1994**, *94*, N°1. (d) Marder, S. R.; Beratan, D. N.; Cheng, L. T. *Science* **1991**, *252*, 103.

(3) Williams D. J. *Ang. Chem. Int. Ed. Engl.* **1984**, *23*, 690.

(4) Eaton, D. F. *Science* **1991**, *253*, 281.

(5) Eich, M.; Bjorklund, G. C.; Yoon, D. Y. *Polym. Adv. Technol.* **1990**, *1*, 189.

(6) *Nonlinear Optical Effects in Organic polymers*; Messier, J., Kazar, F., Prasad, P., Ulrich, D., Ed.; Kluwer Academic Publishers: Dordrecht, 1989.

(7) Dalton, L. R.; Sapochak, L. S.; Chen, M.; Lu, L. P. in *Molecular Electronics and Molecular Electronics devices*; Sienicki, K., Ed.; CRC Press: Boca Raton, FL, 1992; p 125.

(8) (a) Pecaut, J; Masse, R. *Acta Crystallogr.* **1993**, *B49*, 277. (b). Zyss, J.; Masse, R.; Bagiue-Beucher, M.; Levy, J. P. *Adv. Mater.* **1993**, *5*, 120. (c) Kotler, Z.; Hierle, R; Josse, D.; Zyss, J.; Masse, R. *J. Opt. Soc. Am. B.* **1992**, *9*, 534. (d). Masse, R.; Zyss, J. *Mol. Eng.* **1991**, *1*, 141.

(9) (a) Aakeröy, C. B.; Bahra, G. S.; Hitchcock, P. B.; Patell, Y.; Seddon, K. R. *J. Chem. Soc., Chem. Commun.* **1993**, 152. (b) Aakeröy, C. B.; Hitchcock, P. B.; Seddon, K. R. *J. Chem. Soc., Chem. Commun.* **1992**, 553. (c) Aakeröy, C. B.; Hitchcock, P. B.; Moyle, B. D.; Seddon, K. R. *J. Chem. Soc., Chem. Commun.* **1989**, 1856.

(10) Etter, M. C.; Huang, K. S.; *Chem. Mater.* **1992**, *4*, 824.

S0897-4756(97)00692-3 CCC: $15.00
Published on Web 03/04/1998

acid, which is a good starting point as its chirality guarantees a nonlinear response in its salts.[9b,10−12]

The goal of the present contribution is to target the possibility to obtain both efficient chromophore (large β) and alignment (large χ^2) in only one step: the simple neutralization of a stilbazole derivative by L-tartaric acid. INDO calculations performed on crystallographic data and electronic properties are used to provide evidences of large enhancement of the molecular NLO response after protonation, while the alignment in the chiral chain of tartrate ensures an observable bulk effect. The starting dimethylaminostilbazole (DAS) material is shown below.

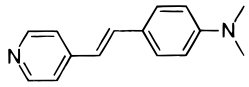

DAS

Experimental Section

Starting Materials and Equipment. Dimethylaminostilbazole (DAS) and dimethylamino-*N*-methylstilbazolium iodide ($DAMS^+I^-$) were synthesized as previously reported,[14] and L-tartaric acid (Janssen Chimica) was used without further purification. ^{1}H NMR spectra were recorded on a Bruker AM 250 spectrometer and UV−visible spectra on a Hewlett-Packard 8452 A spectrophotometer. Elemental analyses were performed by the Service de Microanalyses du C.N.R.S., Laboratoire de Chimie de Coordination, Toulouse.

Synthesis of Diaminostilbazolium Hydrogen Tartrate (DAS-H$^+$ Ta$^-$). In a solution of 336 mg of DAS (1.5×10^{-3} mol) in 100 mL of hot ethanol was added 3.4 g (15-fold excess) of L-tartaric acid in solution in 100 mL of ethanol. Slow evaporation affords orange-red crystals of dimethylaminostilbazolium hydrogen tartrate (yield 85%). Anal. Calcd (found) for $C_{19}H_{22}N_2O_6$: C, 60.95 (60.47); H, 5.92 (5.56); N, 7.48 (7.43).

X-ray Structure Determinations. Single crystals of DAS were grown by slow evaporation from a solution in ethanol, while single crystals of DAS-H^+Ta^- were obtained by recrystallization of the crude material in a solution of tartaric acid (2×10^{-1} mol l^{-1}) in ethanol. The data for compound DAS were collected on a Stoe imaging plate diffraction system (IPDS). The crystal-to-detector distance was 80 mm. 143 exposures (4 min per exposure) were obtained with $0 < \varphi < 200.2°$ and with the crystals rotated through 1.4° in φ. Coverage of the unique set was over 89% complete to at least 24.2°. Crystal decay was monitored by measuring 200 reflections per image. The final unit cell parameters were obtained by the least-squares refinement of 5000 reflections. The data for compound DAS-H^+Ta^- were collected on an Enraf-Nonius CAD4 four-circle diffractometer. The final unit cell parameters were obtained by the least-squares of the setting angles of 25 well-centered reflections. Only statistical fluctuations were observed in the intensity monitors over the course of the data collection. Owing to the rather low μx values, 0.012 and 0.041 calculated for 1 and 2, respectively, no absorption corrections were considered.

The structures were solved by direct methods (SIR92)[15] and refined by least-squares procedures on Fobs. H atoms were located on difference Fourier maps, but those attached to C atoms were introduced into calculation in idealized positions (d(CH) = 0.96 Å) and their atomic coordinates were recalculated after each cycle. They were given isotropic thermal parameters 20% higher than those of the carbon to which they are attached. The coordinates of the H atoms attached to the O atoms were refined with an equivalent isotropic thermal parameter. Least-squares refinements were carried out by minimizing the function $\Sigma w(|F_o| - |F_c|)^2$, where F_o and F_c are the observed and calculated structure factors. The weighting scheme used in the last refinement cycles was $w = w'[1 - (\Delta F/6\sigma(F_o)^2]^2$ where $w' = 1/\Sigma_1^n A_r T_r(x)$ with 3 coefficients A_r for the Chebyshev polynomial $A_r T_r(x)$ where x was F_c/F_c(max).[16] Details of data collection and refinement are given in Table 1.

Table 1. Data Collection and Refinement for DAS and DAS-H$^+$ Ta$^-$

compound	DAS	DAS-H^+Ta^-
formula	$C_{15}H_{16}N_2$	$C_{19}H_{22}N_2O_6$
fw, g	224.31	374.39
shape (color)	flat (yelllow)	flat (orange)
size, mm	0.53, 0.20, 0.08	0.63, 0.45, 0.10
crystal system	monoclinic	monoclinic
space group	$P2_1/c$	$P2_1$
a, Å	6.0443(9)	7.518(1)
b, Å	7.6616(8)	7.528(1)
c, Å	26.376(4)	16.376(2)
β, °	93.66(1)	92.67(1)
V, Å^3	1218.5(3)	925.9(3)
Z	4	2
temperature, K	293(2)	293(2)
radiation	Mo Kα (λ = 0.710 73 Å)	Mo Kα (λ = 0.710 73) Å)
ρ(calcd), g cm^{-3}	1.222	1.343
μ(Mo Kα), cm^{-1}	0.679	0.942
$R(F_o)^a$	0.0445	0.0282
$R_w(F_o)^a$	0.0507	0.0325

^{a} $R = \Sigma(||F_o| - |F_c||)/\Sigma(|F_o|)$. $R_w = \Sigma w(|F_o| - |F_c|)^2/\Sigma w(F_o)^2]^{1/2}$.

The calculations were carried out with the CRYSTALS package programs[17] running on a PC. The drawings of the molecule were realized with the help of CAMERON.[18] The atomic scattering factors were taken from International Tables for X-ray Crystallography. Full X-ray data, fractional atomic coordinates, and the equivalent thermal parameters for all atoms and anisotropic thermal parameters for non-hydrogen atoms have been deposited at the Cambridge Crystallographic Data Center.

Semiempirical Computations. The calculation of electronic transitions for DAS and DAS-H^+ was performed using the INDO/1 Hamiltonian[19] incorporated in the commercially available CAChe work system (Oxford Molecular). The monoexcited configuration interaction (MECI) approximation was employed to describe the excited states. The 81 energy transitions between the nine highest occupied molecular orbitals and the nine lowest unoccupied ones were chosen to undergo CI mixing.

NLO Measurements. The measurements of second-harmonic generation (SHG) intensity were carried out by the Kurtz−Perry powder technique,[20] using a picosecond Nd:YAG pulsed (10 Hz) laser operating at $\lambda = 1.064\ \mu$m. The outcoming Stokes-shifted radiation at 1.907 μm generated by Raman effect in a hydrogen cell was used as the fundamental beam for second-harmonic generation. The SHG signal was detected by a photomultiplier and read on an ultrafast Tektronic 7834

(11) Fuller, J.; Carlin, R. T.; Simpson, L. J.; Furtak, T. E. *Chem. Mater.* **1995**, *7*, 909.
(12) (a) Renuka, K.; Guru Row: T. N.; Prasad, B. R.; Subramanian, C. K.; Bhattacharya, S. *New J. Chem.* **1995**, *19*, 83. (b) Dastidar, P.; Guru Row, T. N.; Prasad, B. R.; Subramanian, C. K.; Bhattacharya, S. *J. Chem. Soc., Perkin Trans. 2* **1993**, 2419.
(13) Pan, F.; Wong, M. S.; Gramlich, V.; Bosshard, C.; Günter, P. *J. Chem. Soc., Chem. Commun.* **1996**, 1557.
(14) Kung, T. K. *J. Chin. Chem. Soc.* **1978**, *25*, 131.
(15) Altomare, A.; Cascarano, G.; Giacovazzo, G.; Guagliardi, A.; Burla, M. C.; Polidori, G.; Camalli, M. SIR92 − a program for automatic solution of crystal structures by direct methods. *J. Appl. Crystallogr.* **1994**, *27*, 435.
(16) Prince, E. *Mathematical Techniques in Crystallography*; Springer-Verlag: Berlin, 1982.
(17) Watkin, D. J.; Prout, C. K.; Carruthers, J. R.; Betteridge, P. W. *CRYSTALS Issue 10*, Chemical Crystallography Laboratory, University of Oxford, Oxford, 1996.
(18) Watkin, D. J.; Prout, C. K.; Pearce, L. J. *CAMERON*, Chemical Crystallography Laboratory, University of Oxford, Oxford, 1996.
(19) Pople, J. A.; Beveridge, D. L. *Approximate Molecular Orbital Theory*; McGraw-Hill Book Company: New York, 1970.
(20) (a) Kurtz, S. K.; Perry, T. T. *J. Appl. Phys.* **1968**, *39*, 3798. (b) Dougherty, J. P.; Kurtz, S. K. *J. Appl. Crystallogr.* **1976**, *9*, 145.

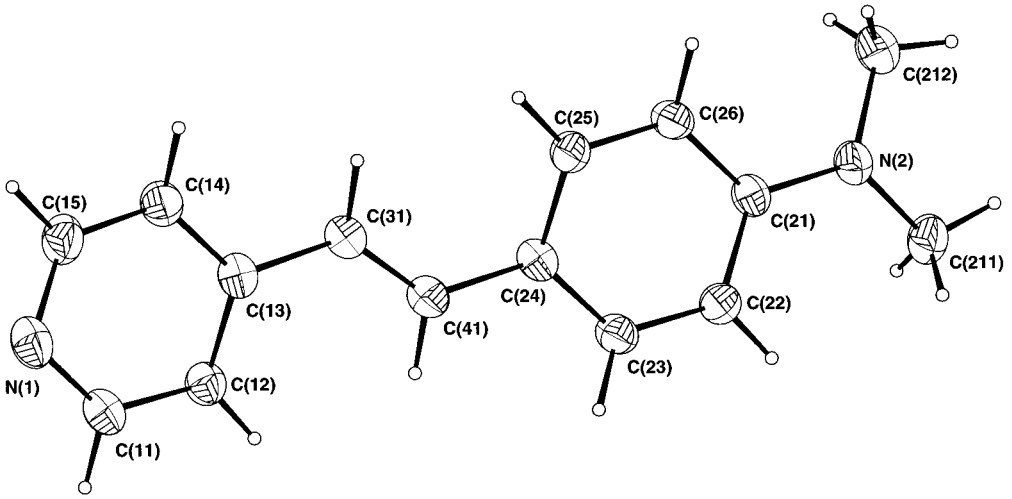

Figure 1. Atom-labeling scheme for DAS.

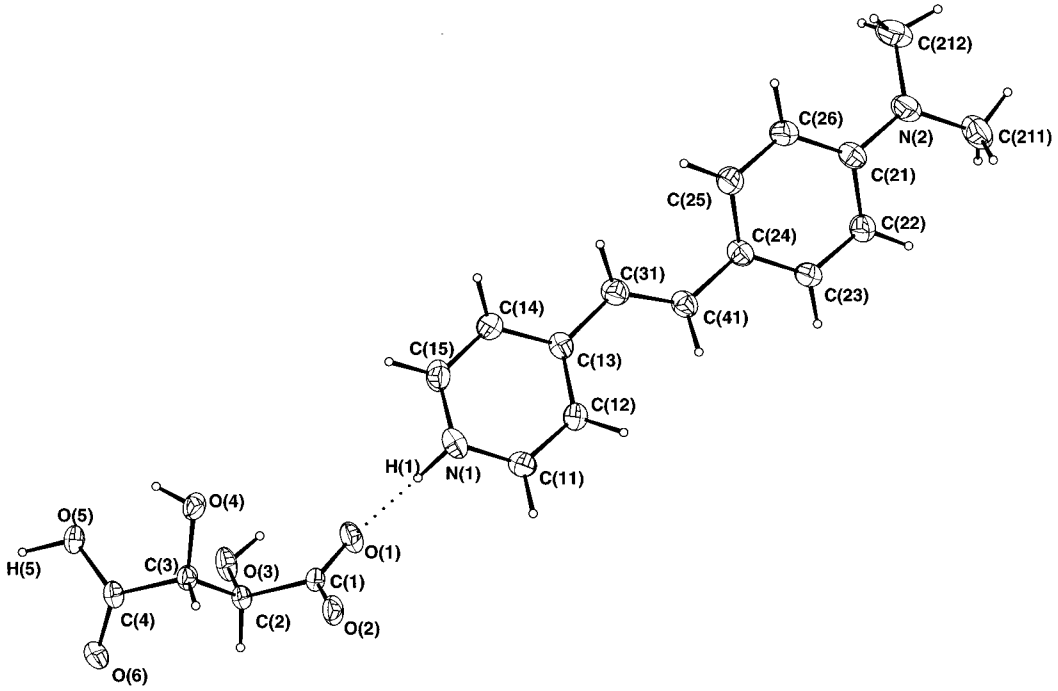

Figure 2. Atom-labeling scheme for DAS-H^+Ta^-.

oscilloscope. Samples were calibrated microcrystalline powders obtained by grinding in the range 50−80 μm and put between two glass plates. The recorded efficiencies were expressed versus that of powdered (50−80 μm) urea.

Results and Discussion

Description of Structures. Figure 1 illustrates the DAS molecule with the atomic numbering scheme employed. The molecule is planar, the largest deviation of −0.128 Å being observed at the C(212) atom. A view of DAS-H^+Ta^- pointing out the hydrogen bond between the dimethylaminostilbazolium and the tartrate with the atomic numbering scheme employed is shown in Figure 2. Figure 3 illustrates the hydrogen-bonded catemer network. As in the neutral DAS molecule, the cation molecule is planar with the largest deviation of 0.102 Å observed at C(211). Selected bond lengths and angles are gathered in Table 2 for DAS and DAS-H^+. The comparison of the geometry between the two molecules reveals slight differences within the dimethylamino group, indeed the nitrogen atom in the DAS molecule retains a pyramidal geometry Σ(CNC) = 358.3° whereas in the protonated molecule the nitrogen atom is planar Σ(CNC) = 359.9°. This result accounts for nitrogen lone-pair delocalization with electron redistribution along the molecule. A slight decreasing from 1.378(3) to 1.366(3) Å in the C−N bond between the amino group and the phenyl ring sustains this view. The difference in bond lengths in the ethenyl fragment between the C(13)−C(31) and C(41)−C(24) single bonds and the C(31)−C(41) double bond is reduced from 0.1455 to 0.1165 Å after protonation. This change is indicative of a higher conjugation and hence a higher quadratic hyperpolarizability for DAS-H^+ in agreement with the bond length alternation (BLA) parameter discussed by Marder.[21]

Molecular Hyperpolarizability (β) of DAS in the Presence of Tartaric Acid. The purpose of this section is to show that DAS engineered into chains of tartrates exhibits molecular properties closely related

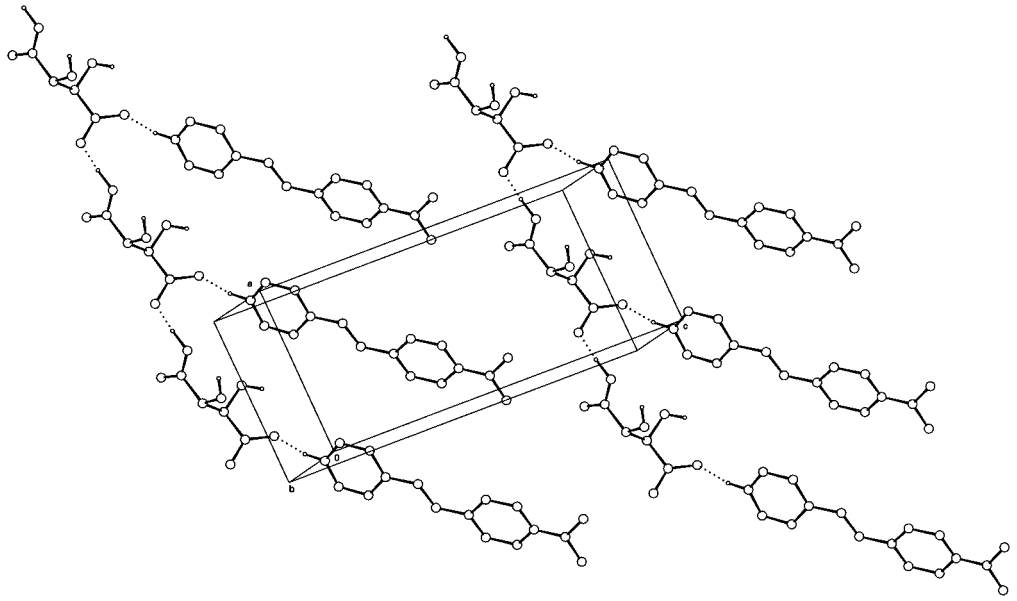

Figure 3. Crystal structure of DAS-H^+Ta^- showing the DAS chromophores hydrogen bonded to the chiral hydrogen tartrate chains.

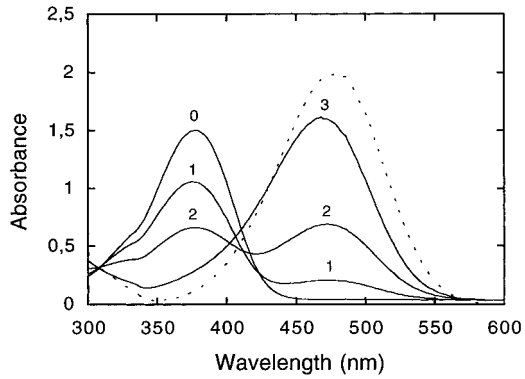

Figure 4. Electronic spectra of DAS (5×10^{-5} mol l^{-1}) in EtOH solution containing different concentrations of tartaric acid: 0 mol l^{-1} (0), 10^{-3} mol l^{-1} (1), 10^{-2} mol l^{-1} (2), 10^{-1} mol l^{-1}(3). The dotted line is $DAMS^+I^-$ (5×10^{-5} mol l^{-1}) in EtOH.

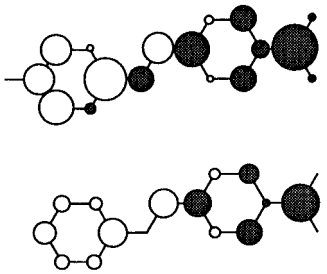

Figure 5. Difference in electronic populations between the ground state and the excited state for the low-lying optical transition (1 → 2) for DAS-H^+ (top) and DAS (bottom). The white (black) contribution is indicative of an increase (decrease) in electron density in the charge-transfer process.

to those of $DAMS^+$, one of the most efficient stilbene-based NLO chromophores. First the ^1H NMR spectra of DAS in a tartaric acid media reported in Table 3 must be considered. It is clear that the chemical shifts recorded are more similar to those observed for $DAMS^+$ than those recorded for neutral DAS. However, this effect accounts for the electronic ground state only. More important are the UV−visible spectra of DAS recorded in ethanol containing various amounts of tartaric acid (Figure 4). It can be easily observed that both DAS-H^+Ta^- and $DAMS^+$ exhibit similar intense low-lying transitions located at 468 nm ($\epsilon = 32300$ mol^{-1} cm^{-1}) and 478 nm ($\epsilon = 39600$ mol^{-1} cm^{-1}), respectively, while it is observed at 377 nm ($\epsilon = 30100$ mol^{-1} cm^{-1}) for DAS. It has long been recognized that the longest wavelength absorption band of disubstituted benzene derivatives is responsible for the second-order NLO response of the molecule, according to the well-known and widely used "two-level model".[22] In this model, the hyperpolarizability (β) can be described in terms of a ground and a first excited state having charge-transfer character and is related to the energy of the optical transition (E), its oscillator strength (f), and the difference between ground- and excited-state dipole moments ($\Delta\mu$) through the relation:

$$\beta \propto f\Delta\mu/E^3$$

The effects of substituent patterns on the hyperpolarizability of a chromophore are readily correlated with the electron-donating and -accepting strength of the substitutents. In other words, the protonation of DAS by tartaric acid is expected to enlarge the NLO response by increasing the intramolecular charge transfer and lowering its energy, as a pyridinium (or *N*-methylpyridinium in the case of $DAMS^+$) is a better acceptor unit than a pyridine.

INDO-calculated data are reported in Table 4 for the low-lying transitions of DAS and DAS-H^+. First, it should be pointed out that both compounds exhibit only one intense transition (large oscillator strength), principally involving the HOMO → LUMO transition, in good agreement with the electronic spectra. The role devoted to stilbazole protonation can be evidenced in

(21) (a) Marder, S. R.; Gorman, C. B.; Meyers, F.; Perry, J. W.; Bourhill, G.; Brédas, J. L.; Pierce, B. M. *Science* **1994**, *265*, 632. (b) Meyers, F.; Marder, S. R.; Pierce, B. M.; Brédas, J. L. *J. Am. Chem. Soc.* **1994**, *116*, 10703.

(22) (a) Oudar, J. L.; Chemla, J. *J. Chem. Phys.* **1977**, *66*, 2664. (b) Oudar, J. L. *J. Chem. Phys.* **1977**, *67*, 446.

Table 2. Comparison of Bond Lengths (Å) and Bond Angles (deg) within the Neutral DAS and Protonated DAS-H$^+$[a]

DAS		DAS-H$^+$	
	Bond Lengths		
N(1)−C(11)	1.332(3)	N(1)−C(11)	1.332(3)
N(1)−C(15)	1.333(3)	N(1)−C(15)	1.336(3)
		N(1)−H(1)	0.96(2)
N(2)−C(21)	1.378(3)	N(2)−C(21)	1.366(3)
N(2)−C(211)	1.439(3)	N(2)−C(211)	1.442(3)
N(2)−C(212)	1.436(3)	N(2)−C(212)	1.431(3)
C(11)−C(12)	1.371(3)	C(11)−C(12)	1.357(3)
C(12)−C(13)	1.397(3)	C(12)−C(13)	1.390(3)
C(13)−C(14)	1.382(3)	C(13)−C(14)	1.395(3)
C(13)−C(31)	1.472(3)	C(13)−C(31)	1.452(3)
C(14)−C(15)	1.370(3)	C(14)−C(15)	1.362(3)
C(21)−C(22)	1.394(3)	C(21)−C(22)	1.402(3)
C(21)−C(26)	1.411(3)	C(21)−C(26)	1.401(3)
C(22)−C(23)	1.376(3)	C(22)−C(23)	1.374(3)
C(23)−C(24)	1.390(3)	C(23)−C(24)	1.390(3)
C(24)−C(25)	1.398(3)	C(24)−C(25)	1.393(3)
C(24)−C(41)	1.459(3)	C(24)−C(41)	1.451(3)
C(25)−C(26)	1.369(3)	C(25)−C(26)	1.370(3)
C(31)−C(41)	1.320(3)	C(31)−C(41)	1.335(3)
	Bond Angles		
C(11)−N(1)−C(15)	115.1(2)	C(11)−N(1)−C(15)	121.2(2)
C(11)−N(1)−C(15)		C(11)−N(1)−H(1)	119.2(15)
C(11)−N(1)−C(15)		C(15)−N(1)−H(1)	119.4(14)
C(21)−N(2)−C(211)	120.6(2)	C(21)−N(2)−C(211)	121.1(2)
C(21)−N(2)−C(212)	120.5(2)	C(21)−N(2)−C(212)	121.4(2)
C(211)−N(2)−C(212)	117.2(2)	C(211)−N(2)−C(212)	117.4(2)
N(1)−C(11)−C(12)	124.6(2)	N(1)−C(11)−C(12)	120.4(2)
C(11)−C(12)−C(13)	119.9(2)	C(11)−C(12)−C(13)	120.9(2)
C(12)−C(13)−C(14)	115.5(2)	C(12)−C(13)−C(14)	116.5(2)
C(12)−C(13)−C(31)	124.3(2)	C(12)−C(13)−C(31)	123.9(2)
C(14)−C(13)−C(31)	120.2(2)	C(14)−C(13)−C(31)	119.7(2)
C(13)−C(14)−C(15)	120.3(2)	C(13)−C(14)−C(15)	120.7(2)
N(1)−C(15)−C(14)	124.6(2)	N(1)−C(15)−C(14)	120.2(2)
N(2)−C(21)−C(22)	122.2(2)	N(2)−C(21)−C(22)	121.6(2)
N(2)−C(21)−C(26)	121.2(2)	N(2)−C(21)−C(26)	121.6(2)
C(22)−C(21)−C(26)	116.6(2)	C(22)−C(21)−C(26)	116.8(2)
C(21)−C(22)−C(23)	121.1(2)	C(21)−C(22)−C(23)	121.1(2)
C(22)−C(23)−C(24)	122.8(2)	C(22)−C(23)−C(24)	122.2(2)
C(23)−C(24)−C(25)	115.8(2)	C(23)−C(24)−C(25)	116.4(2)
C(23)−C(24)−C(41)	120.2(2)	C(23)−C(24)−C(41)	119.8(2)
C(25)−C(24)−C(41)	124.0(2)	C(25)−C(24)−C(41)	123.7(2)
C(24)−C(25)−C(26)	122.4(2)	C(24)−C(25)−C(26)	122.3(2)
C(21)−C(26)−C(25)	121.2(2)	C(21)−C(26)−C(25)	121.2(2)
C(13)−C(31)−C(41)	126.8(2)	C(13)−C(31)−C(41)	125.2(2)
C(24)−C(41)−C(31)	127.1(2)	C(24)−C(41)−C(31)	127.6(2)

[a] Esd's in parentheses refer to the last significant digit.

Table 3. ^{1}H NMR Data[a] for Dimethylaminostilbazole (DAS), Dimethyl aminostilbazolium Hydrogen Tartrate (DAS-H$^+$Ta$^-$), and Dimethylamino-*N*-methylstilbazolium Iodide (DAMS$^+$I$^-$) in CD_3OD

DAS	DAS-H$^+$Ta$^-$	DAMS$^+$I$^-$
8.486 (d, 2H, 6.3 Hz)	8.638 (d, 2H, 6.7 Hz)	8.603 (d, 2H, 7.0 Hz)
7.590 (d, 2H, 6.2 Hz)	8.076 (d, 2H, 6.7 Hz)	8.063 (d, 2H, 7.0 Hz)
7.573 (d, 2H, 9.0 Hz)	7.702 (d, 2H, 8.9 Hz)	7.704 (d, 2H, 9.0 Hz)
7.491 (d, 1H, 16.3 Hz)	7.903 (d, 1H, 16.0 Hz)	7.933 (d, 1H, 16.0 Hz)
6.999 (d, 1H, 16.3 Hz)	7.180 (d, 1H, 16.0 Hz)	7.185 (d, 1H, 16.0 Hz)
6.854 (d, 2H, 8.9 Hz)	6.884 (d, 2H, 9.0 Hz)	6.880 (d, 2H, 9.0 Hz)
3.028 (s, 6H)	3.146 (s, 6H)	3.160 (s, 6H)
		4.311 (s, 3H)

[a] Chemical shift (mutiplicity, intensity, coupling constant).

Figure 5, where the difference in electronic populations between the ground and excited state is shown for the low-lying transition (1 → 2) of both compounds. As anticipated, the pyridine moieties act as a modest acceptor unit in DAS, while an enhancement of the withdrawing effect is observed for the pyridinium fragment. λ_{max} is shifted to lower energy, $\Delta\mu$ is enlarged, and hence the hyperpolarizability is enlarged. Using the two-level description and the data given in Table 4, the hyperpolarizability of DAS-H$^+$ is expected to be five times that of DAS.

Bulk Susceptibility of DAS Engineered into Acentric Tartrate Chains. The relationship between microscopic and macroscopic second-order optical nonlinearities has been extensively investigated for any noncentrosymmetric crystal point group.[23] The hyperpolarizability tensor (components β_{ijk} in the molecular frame) is related to the corresponding crystalline first-order nonlinearity χ^2 (components d_{IJK} in crystalline frame) through the following relation:

$$d_{IJK}(-2\omega;\omega,\omega) = N f_I^{2\omega} f_J^{\omega} f_k^{\omega} \times \sum \cos(I,i)\cos(J,j)\cos(K,k)\beta_{ijk}$$

N is the number of chromophores per unit volume; $f_I^{2\omega}$, f_J^{ω}, and f_K^{ω} are Lorentz local-field factors. The summation is performed over all molecules in the unit cell, and the cosine product terms represent the rotation from the molecular reference frame into the crystal frame. The molecules presented in our paper crystallize in space group $P2_1$ (monoclinic point group 2). Assuming a simplified one-dimensional description of the molecular nonlinear tensor of the molecules, β has only one nonvanishing coefficient along the charge-transfer axis x of the molecule (namely β_{xxx}). This model leads to

$$d_{YXX} = N\beta_{xxx}\cos\theta\sin^2\theta$$

$$d_{YYY} = N\beta_{xxx}\cos^3\theta$$

all other components of the tensor are neglectible (θ is defined as the angle between the main intramolecular charge-transfer axis ox and the 2-fold axis OY of the crystal). It is obvious from the expression of d_{YXX} and d_{YYY} that the situation with $\theta = 90°$ will lead to a cancellation of the nonlinearity for the bulk material and must therefore be avoided. In the case of our derivative, θ reaches a value of 87.93° which gives an angular factor of 0.036 for d_{YXX}, far from the maximized 0.385 value obtained for $\theta = 54.74°$. DAS-H$^+$Ta$^-$ was found to exhibit an efficiency 8 times that of urea in second-harmonic generation at 1.907 μm, while DAS exhibits no efficiency, due to centrosymmetry.

As is well-known, chirality provides the synthetic chemist with a means of guaranteeing that crystallization of a pure enantiomer will occur in a noncentrosymmetric point group. However, the fact that a molecule is optically pure does not guarantee that the molecular packing will be optimized for NLO effects. In the case of DAS-H$^+$Ta$^-$, the charge-transfer system crystallizes in a quasi antiparallel geometry, thus canceling the major part of β, whereas the chiral groups, which do not contribute significantly to the nonlinearity, form an oriented sublattice of limited relevance for nonlinear optics.

Conclusion

Most chromophores that have been examined for second-order nonlinear properties have dipole moments and approximately linear shapes, which apparently

(23) Zyss, J.; Oudar, J. L. *Phys. Rev. A* **1982**, *26*, 2028.

Table 4. Energies (λ_{max} in nm), Oscillator Strengths (f), Dipole Moment Changes between Ground and Excited States ($\Delta\mu$ in D), and Composition of the First Excited States of DAS and DAS-H$^+$

compd	transition	λ_{max}	f	$\Delta\mu$	composition of CI expansion
DAS	1 → 2	317	1.29	14.8	$0.954\chi_{43\rightarrow44} - 0.165\chi_{43\rightarrow46} + 0.148\chi_{42\rightarrow46} + 0.125\chi_{42\rightarrow44}$
	1 → 3	302	0.05	2.0	$-0.852\chi_{43\rightarrow45} - 0.342\chi_{40\rightarrow44} + 0.289\chi_{40\rightarrow46} + 0.129\chi_{40\rightarrow48}$
	1 → 4	280	0.01	17.2	$0.730\chi_{39\rightarrow44} + 0.510\chi_{39\rightarrow46} - 0.305\chi_{39\rightarrow48} + 0.227\chi_{39\rightarrow47} + 0.186\chi_{39\rightarrow50}$
DAS-H$^+$	1 → 2	476	1.09	−26.0	$0.937\chi_{43\rightarrow44} - 0.250\chi_{41\rightarrow44} + 0.209\chi_{43\rightarrow46} + 0.057\chi_{41\rightarrow48}$
	1 → 3	317	0.01	−30.6	$0.914\chi_{43\rightarrow45} - 0.348\chi_{41\rightarrow45} - 0.115\chi_{39\rightarrow44}$
	1 → 4	314	0.00	−13.3	$-0.649\chi_{43\rightarrow47} + 0.618\chi_{42\rightarrow44} + 0.377\chi_{42\rightarrow46} + 0.143\chi_{42\rightarrow48}$

cause most of them to crystallize in centrosymmetric space groups. A strategy employed first by Meredith[24] involves the use of ionic chromophores to encourage noncentrosymmetric crystallization. Systematic structural investigations of classes of SHG materials have been already carried out for various salts including dihydrogenophosphate,[9] aminonitropyridinium,[25] stilbazolium,[26] and nitroaniline salts.[27] These studies were aimed at correlating structural properties to the nonlinear responses, targeting a possible "tuning" of the structure to enhance the NLO response. On the other hand, the electronic properties of the chromophore were not affected during the engineering process. In our study, the neutralization of substituted stilbazole base by L-tartaric acid enhanced the NLO response at the molecular (β) and bulk (χ^2) levels simultaneously. We have provided evidences for a large hyperpolarizability, while progress has to be made now to optimize the geometric orientation of the chromophores in the crystal.

Supporting Information Available: Tables of crystal data, fractional atomic coordinates, anisotropic thermal parameters, bond lengths, and bond angles for the DAS and DAS-H$^+$Ta$^-$ (6 pages). Ordering information is given on any current masthead page.

CM970692Z

(24) Meredith, G. In *Nonlinear Optical Properties of Organic and Polymeric Materials*; Williams, D. J., Ed.; ACS Symposium Series 233; Washington, DC, 1983, p 27.

(25) (a) Pecaut, J; Masse, R. *Acta Crystallogr.* **1993**, *B49*, 277. (b) Masse, R.; Zyss, J. *Mol. Eng.* **1991**, *1*, 141. (c) Kotler, Z.; Hierle, R; Josse, D.; Zyss, J.; Masse, R. *J. Opt. Soc. Am. B.* **1992**, *9*, 534.

(26) (a) Marder, S. R.; Perry, J. W.; Schaefer, W. P. *Science* **1989**, *245*, 626. (b) Marder, S. R.; Perry, J. W.; Tieman, B. G.; Marsh, R. E.; Schaefer, W. P. *Chem. Mater.* **1990**, *2*, 685.

(27) Gotoh, T.; Mizuno, N.; Iwamoto, M.; Hashimoto, S.; Kawasaki, M.; Hashimoto, M.; Misono, M. *Chem. Mater.* **1992**, *4*, 502.